INTERNATIONAL JOURNAL OF CLIMATOLOGY
Int. J. Climatol. **24**: 1091–1107 (2004)
Published online in Wiley InterScience (www.interscience.wiley.com). DOI: 10.1002/joc.1044

DIFFERENCES IN RAINFALL VARIABILITY IN THE SOUTH AND SOUTHEAST ASIAN SUMMER MONSOONS

IGOR I. ZVERYAEV[a,*] and MARINA P. ALEKSANDROVA[b]
[a] *P.P. Shirshov Institute of Oceanology, RAS, Moscow, Russia*
[b] *Department of Meteorology, Faculty of Geography, Moscow State University, Moscow, Russia*

Received 25 June 2003
Revised 3 March 2004
Accepted 3 March 2004

ABSTRACT

Long-term rainfall variability in the South and Southeast Asian summer monsoons is investigated using observational data for a 50 year period. Linear trends indicate a general level of summer rainfall decrease over northeast India that has intensified during recent decades. In contrast to the South Asian Monsoon (SAM), there is no significant rainfall trend in the Southeast Asian Monsoon (SEAM).

The result of the empirical orthogonal functions (EOFs) analysis has shown that the leading EOF modes explain about 25% of total rainfall variability in both regions. Low correlation between respective principal components implies that rainfall variations in the two monsoon subsystems are not related, suggesting that different mechanisms are responsible for the interannual rainfall variability in the SAM and the SEAM.

The interannual variability of the SAM rainfall is linked to sea-surface temperature (SST) fluctuations in the equatorial eastern Pacific during the monsoon season and the following autumn. As revealed by lead–lag correlations, the warming of the Arabian Sea and a region located northwest of Australia during the boreal winter may lead to a strong SAM. The interannual behaviour of the SAM rainfall shows a feature of the quasi-biennial oscillation with the reversal of correlations between months preceding the monsoon and the monsoon–post-monsoon months. In comparison with the SAM, the interannual variability of the SEAM rainfall is associated with distinctly different SST patterns. Enhanced SEAM rainfall is preceded by a high SST in the northern Indian Ocean and the South China Sea in the previous January and February. Significant correlations between the SEAM rainfall and SST, which form a tripole pattern in the North Pacific Ocean, are detected during the preceding winter and early spring, suggesting that wintertime tropics–extratropics interactions may play a role in the SEAM rainfall variability. Copyright © 2004 Royal Meteorological Society.

KEY WORDS: South Asia; Southeast Asia; linear trends; empirical orthogonal functions; rainfall

1. INTRODUCTION

Being a key element of the global climate system, the Asian monsoon influences most of the tropics and subtropics of the Eastern Hemisphere (Webster *et al*., 1998). There is also evidence that the monsoon may influence the atmospheric circulation in the extratropics. The Asian summer monsoon displays a pronounced variability on a wide range of time scales from intraseasonal to interannual and interdecadal (Chang and Krishnamurti, 1987; Fein and Stephens, 1987; Webster *et al*., 1998). Interannual variability in the rainfall intensity during the summer monsoon season over South and Southeast Asia leads to significant economic and social consequences (Parthasarathy *et al*., 1988; Gadgil, 1996; Webster *et al*., 1998). A strong monsoon can result in devastating floods, whereas a weak monsoon is usually associated with droughts, thus affecting living conditions and the economy of the densely populated region. Therefore, the correct long-lead prediction of monsoon rainfall is one of major challenges of modern climate research.

* Correspondence to: Igor I. Zveryaev, P.P. Shirshov Institute of Oceanology, RAS 36, Nakhimovsky Ave., Moscow, 117851, Russia; e-mail: igorz@sail.msk.ru

To improve monsoon prediction, many studies have focused on the relationships between the monsoon and the major climatic signal in the tropics, i.e. El Niño–southern oscillation (ENSO). Some of these studies (Webster and Yang, 1992; Ju and Slingo, 1995; Lau and Bua, 1998; Yang and Lau, 1998) suggested that ENSO may have an influence on the interannual variability of the Asian summer monsoon. However, many extreme monsoon droughts and floods were not associated with ENSO (Webster *et al*., 1998). It is worth noting that the monsoon–ENSO relationships are not stable, e.g. Torrence and Webster (1999) and Clark *et al*. (2000) demonstrated that these relationships undergo interdecadal changes. Indeed, as was shown earlier (Normand, 1953; Troup, 1965), contemporaneous relationships between Indian rainfall and ENSO do exist, albeit that a prior knowledge of the ENSO indices during the previous winter or spring does not help in forecasting the summer monsoon. Normand (1953) concluded that the Indian monsoon stands out as an active agent in the monsoon–ENSO relationships and, therefore, is more efficient as a broadcasting tool than an event to be forecast. The predictive relationships between Indian Ocean sea-surface temperature (SST) and monsoon rainfall are less studied. Several studies investigated links between Indian Ocean SST and monsoon variability. Sadhuram (1997) found a strong correlation between Indian summer monsoon rainfall and SST in the central Indian Ocean in the preceding October and November. A strong positive correlation of the spring SST in the Arabian Sea with the Indian summer rainfall was detected in several studies (Shukla and Mooley, 1987; Rao and Goswami, 1988; Allan *et al*., 1995). Nicholls (1983) found significant correlations between the all-India rainfall index (AIRI; see Section 2 and Parthasarathy *et al*. (1992, 1994)) and the Indonesian SST in February preceding the Indian monsoon. Recently, Clark *et al*. (2000) examined relationships between AIRI and the Indian Ocean SST and found strong correlations between the summer AIRI and the preceding winter SST in the Arabian Sea and in a region located northwest of Australia. Very high correlations were also found in the central Indian Ocean in the preceding autumn for the years after 1977, but this relationship was much weaker in earlier years.

We note that the majority of the above studies were focused on the Indian (or South Asian) monsoon (SAM) and its relationships with SST variations. Less attention has been paid so far to the analysis of another important subcomponent of the Asian monsoon system, i.e. the Southeast Asian monsoon (SEAM). Long-term variability of the SEAM and its links to SST variations are not well studied. Though India and Southeast Asia are closely located, and the monsoon onsets occur at almost similar times in the two monsoon subsystems, differences in year-to-year rainfall variability in the SAM and the SEAM were noted in several studies (Lau, 1998; Wang and Fan, 1999; Lau *et al*., 2000). Based on the characteristic monsoon evolution, Lau (1998) suggested distinguishing the SAM and the SEAM subsystems in the tropical Asian monsoon domain. To reflect regional monsoon characteristics better, Wang and Fan (1999) suggested two convection indices to measure the variability of the SAM and the SEAM. More recently, Lau *et al*. (2000) have developed other indices for two major subcomponents of the Asian summer monsoon, and investigated their links to SST variations. They found that interannual variabilities of the SAM and the SEAM are associated with distinctly different SST patterns. To construct the above indices of the SAM and the SEAM variability, Wang and Fan (1999) used the outgoing longwave radiation and Lau *et al*. (2000) used atmospheric circulation data. Thus, it remains interesting to investigate further specific features in the interannual rainfall variability in the two monsoon subsystems, and their relation to SST variations in the Indo-Pacific basin.

In this study, based on relatively new and long-period rainfall and SST data, we examine the spatial–temporal structure of year-to-year summer rainfall variability in the SAM and the SEAM. Then, considering the respective principal components (obtained by applying empirical orthogonal functions (EOFs) analysis) as objectively defined rainfall indices, we investigate links between summer rainfall variability in the SAM and the SEAM and SST variations in the tropical Indian and Pacific Oceans.

The paper is organized as follows. The data used and the analysis methods are described in Section 2. The climatology and general structure of year-to-year summer rainfall variations in the SAM and the SEAM are discussed in Section 3. In Section 4 we use EOFs analysis to examine dominant modes of interannual rainfall variations. Subsequently, their links to major tropical climate indices and to SST variations in the tropical Indian and Pacific oceans are analysed in Section 5. Finally, concluding remarks are given in Section 6.

2. DATA AND METHODS

The basic data set used in this study is the CRU05 0.5° lat/lon gridded monthly climate data (New *et al*., 1999, 2000). This data set has been constructed at the Climatic Research Unit, University of East Anglia, UK. The data set represents terrestrial surface climate for the period 1901–98. This relatively new data set has advanced features over other products: (i) it has higher spatial resolution than other data sets of similar temporal extent; (ii) it has longer temporal coverage than other products of similar spatial resolution; (iii) it encompasses a more extensive suite of surface climate variables than available elsewhere; and (iv) the construction method ensures that strict temporal homogeneity is maintained. In this study we use data on the Indian and Southeast Asian precipitation that were interpolated directly from station observations. Details on the data construction method can be found in New *et al*. (1999, 2000).

Although we performed EOF analysis (and other calculations) for the 1901–98 and 1949–98 time periods, the present study is focused on consideration of the period 1949–98, covered by the most reliable data. The domain of analysis is limited to latitudes 8–32 °N and longitudes 68–90 °E for the SAM, and to latitudes 8–32 °N and longitudes 94–123 °E for the SEAM. The areas are chosen based on considerations of geography and coherent rainfall systems. We note that Krishnamurthy and Shukla (2000) recently performed EOF analysis of the SAM rainfall for the essentially different time period 1901–70. However, to the best of our knowledge, EOF analysis of the SEAM rainfall is performed for the first time in the present study.

In order to assess links between monsoon rainfall and SST variations, we used SST data for the tropical Indian and Pacific Oceans. The SST data were derived from the gridded monthly Global Sea-Ice and SST dataset (GISST, version 2.3b) compiled by the Hadley Centre for Climate Prediction and Research, UK Meteorological Office. The time period corresponding with the precipitation data is used. The SST data have a resolution of 1° latitude by 1° longitude and are quality controlled (Rayner *et al*., 1995; Parker *et al*., 1995). In our study, we use the monthly means from 1949 through to 1998 for the tropical Indian and Pacific Oceans between 30 °N and 30 °S.

In this study, we also use several key tropical climate indices. The AIRI (Parthasarathy *et al*., 1992, 1994) consists of an area-weighted average of 306 rain gauges distributed across India. The index has been computed for the past century and has been widely used as an indicator of the strength of the SAM.

The southern oscillation index (SOI; (Troup, 1965; Trenberth, 1984; Ropelewski and Jones, 1987)) was proposed by Troup (1965) to represent the southern oscillation, i.e. the pressure seesaw over the tropical South Pacific and the tropical Indian sector. Defined as the normalized sea-level pressure anomaly difference between Darwin in Australia, and Tahiti, it has been widely used to measure the ENSO phenomenon.

The Niño 3.4 index (Trenberth, 1997) is another measure of the ENSO phenomenon. The index is constructed by averaging the SST anomaly over the Niño 3.4 region (120–170 °W and 5 °S–5 °N).

Here, we consider the climatology of the summer monsoon season (June–September (JJAS)) mean rainfall and its standard deviation (STD) as a measure of the interannual rainfall variability. To help clarify the definition, we use the term strong/weak monsoon just to characterize monsoon seasons with above-below-normal precipitation. Because we do not consider (calculate) specific characteristics (e.g. composites of precipitation) of the strong/weak monsoons, there is no need for more strict criteria (like a certain threshold level) for the definition of the monsoon strength. To examine the spatial–temporal structure of long-term variations of JJAS rainfall in the SAM and SEAM, we applied EOFs analysis based on the covariance matrix (Wilks, 1995; von Storch and Navarra, 1995). The spatial patterns and respective principal components of the first EOF mode are discussed in detail. Correlation analysis is performed in order to establish links to major tropical climate indices, and to SST variations.

3. RAINFALL CLIMATOLOGIES AND VARIABILITIES OVER INDIA AND SOUTHEAST ASIA

The climatological summer (JJAS) mean rainfall pattern over India (SAM region; Figure 1(a)) demonstrates high (250–300 mm/month) precipitation along the western coast of Indostan, over central and northeastern India near the foothills of the Himalayas. Relatively dry (about 100 mm/month) conditions are observed over

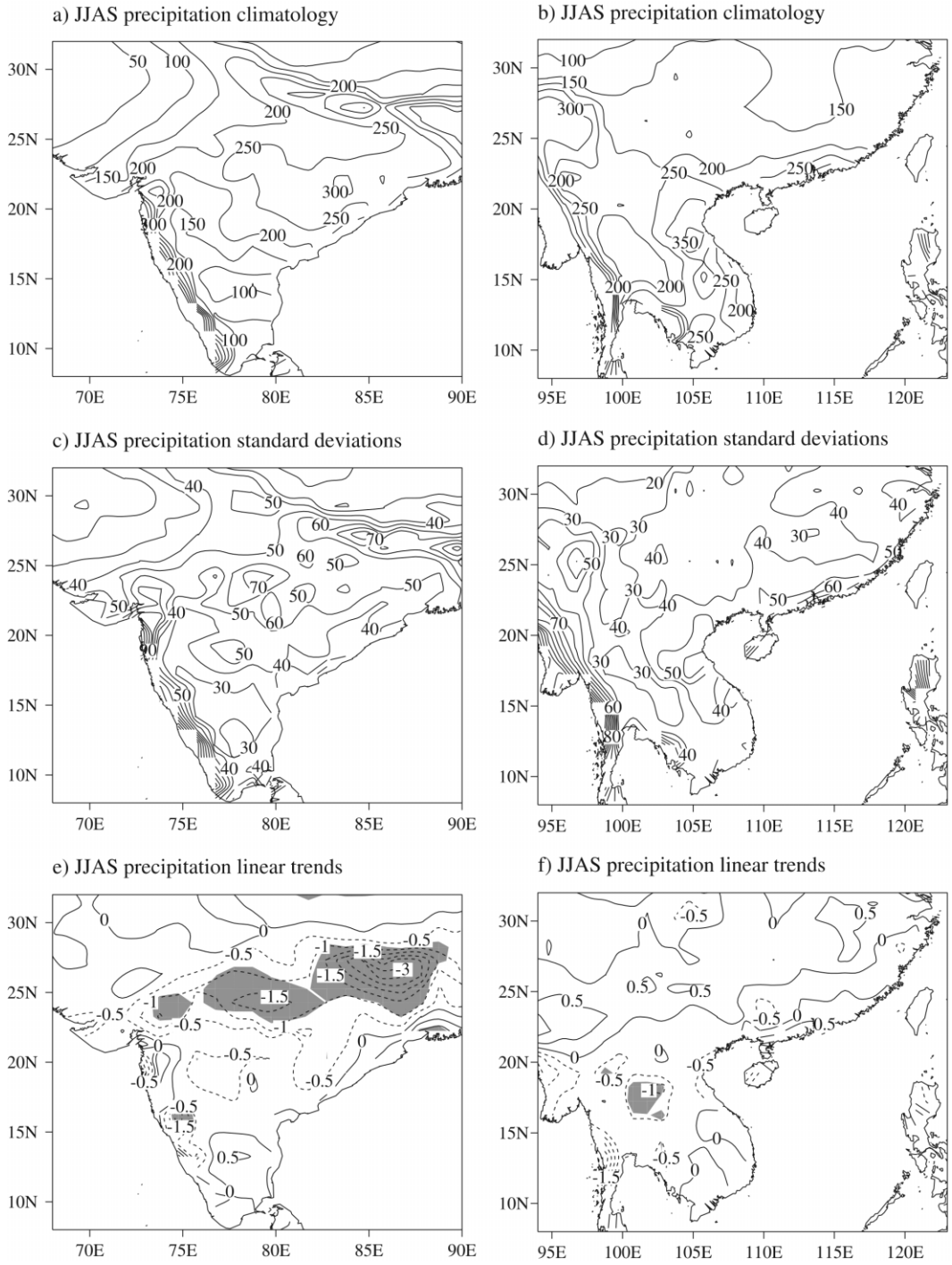

Figure 1. Summer (JJAS) rainfall climatologies of (a) SAM and (b) SEAM, (c, d) their standard deviations, and (e, f) linear trends for 1949–98. Shaded areas indicate confidence level exceeding 95%

northwestern and southeastern India. The STD of time series of JJAS rainfall is a measure of its year-to-year variability (Figure 1(c)). This variability is large (60–80 mm/month) over the regions of high precipitation, and vice-versa (Figure 1(a)). The estimated linear trends (Figure 1(e)) demonstrate a decrease in precipitation

over almost the whole of India during 1949–98. However, according to the Student's *t*-test (Bendat and Piersol, 1966) the trends are statistically significant at the 95% confidence level only over northeastern India. In this region, linear trends indicate a rainfall decrease at the rate of about 3 mm/month per year. We note that the present trends are essentially stronger than those estimated for 1901–98 (not shown), indicating an intensification of long-term precipitation decrease over northeastern India during recent decades.

Figure 1(b) shows the climatology of the JJAS rainfall over Southeast Asia (SEAM region). The largest rainfall amounts exceeding 350 mm/month are found over the coastal regions of Southeast Asia. We note that the maxima of precipitation over Southeast Asia are higher than those over India. Over the northern part of the region the precipitation is essentially lower (about 100–150 mm/month) than that over the coastal regions of Southeast Asia. The spatial structure of the total JJAS rainfall variability over Southeast Asia, represented by its STD, is shown in Figure 1(d). Basically, the distribution of maxima and minima is the same as that of JJAS rainfall climatology (Figure 1(b)). The highest (50–70 mm/month) interannual variability of the JJAS rainfall is observed over the coastal regions, and the lowest rainfall variability is over the central and northern parts of Southeast Asia (Figure 1(d)). As seen in Figure 1(f), in contrast to the SAM, there are no statistically significant long-term rainfall trends in the SEAM. This is consistent with the results presented by Kripalani and Kulkarni (1997), who analysed station rainfall data and did not find systematic climate change or rainfall trends in the region.

4. EOF MODES OF RAINFALL VARIABILITY

To define and analyse the leading modes of the interannual variability of JJAS rainfall in the SAM and the SEAM, we applied EOF analysis to the seasonal mean rainfall time series over the two regions. In order to preserve the long-term stationarity of the time series, prior to the EOF analysis the linear trends were removed from the JJAS rainfall time series.

The spatial patterns of the first EOF modes of the SAM and SEAM rainfall are presented in Figure 2(a) and (b). The time series of the corresponding principal components are shown in Figure 2(c) and (d).

In both these monsoon systems, only the first EOF modes are separated reasonably well with respect to sampling errors (North *et al*., 1982) and are relatively stable. Both in the SAM (Figure 2(a)) and the SEAM (Figure 2(b)), the spatial patterns of the first EOF modes of JJAS rainfall reflect coherent variations over the whole of the respective regions, and are characterized by the largest loadings in the western parts of the respective regions.

The first EOF mode accounts for 25.03% of the total variance of JJAS rainfall over India. The spatial pattern is characterized by coherent rainfall changes over the whole of India, with the largest loadings over central India and along the western coast of Indostan (Figure 2(a)). We note that the first EOF mode estimated for 1901–98 reveals a very similar spatial pattern and corresponding principal components (not shown). However, this mode explains a smaller portion (23.60%) of the total rainfall variance. Therefore, in terms of explained variance, our results suggest a strengthening of the first EOF mode during the last 50 years. This is corroborated by the results of Krishnamurthy and Shukla (2000), who performed EOF analysis of the SAM rainfall for the time period 1901–70 and revealed the first EOF mode had a similar (i.e. reflected coherent rainfall variations over the entire region) spatial structure, but explained a smaller portion (20.70%) of the total rainfall variance in the region. The corresponding principal components (Figure 2(c)) show interannual rainfall variations that are consistent with those detected in AIRI (Parthasarathy *et al*., 1994). In particular, flood (e.g. 1961, 1970, 1975, 1983, 1988, 1994) and drought (e.g. 1951, 1965, 1966, 1968, 1972, 1974, 1987) years detected in AIRI are revealed correctly by the first EOF mode of JJAS rainfall (Figure 2(c)). In fact, as expected, the principal components of the first EOF mode demonstrate a very high (0.91) and statistically significant (at the 99% confidence level) correlation with AIRI.

The first EOF mode explains 24.17% of the total variance of JJAS rainfall over Southeast Asia. Its spatial pattern is characterized by rainfall variations with the strongest signal being in the western part of the region (near the Bay of Bengal; Figure 2(b)). A secondary maximum of variability is seen over the southern coast of China. The first EOF mode from 1901 to 1998 has a similar spatial pattern and explains only 14.21% of the

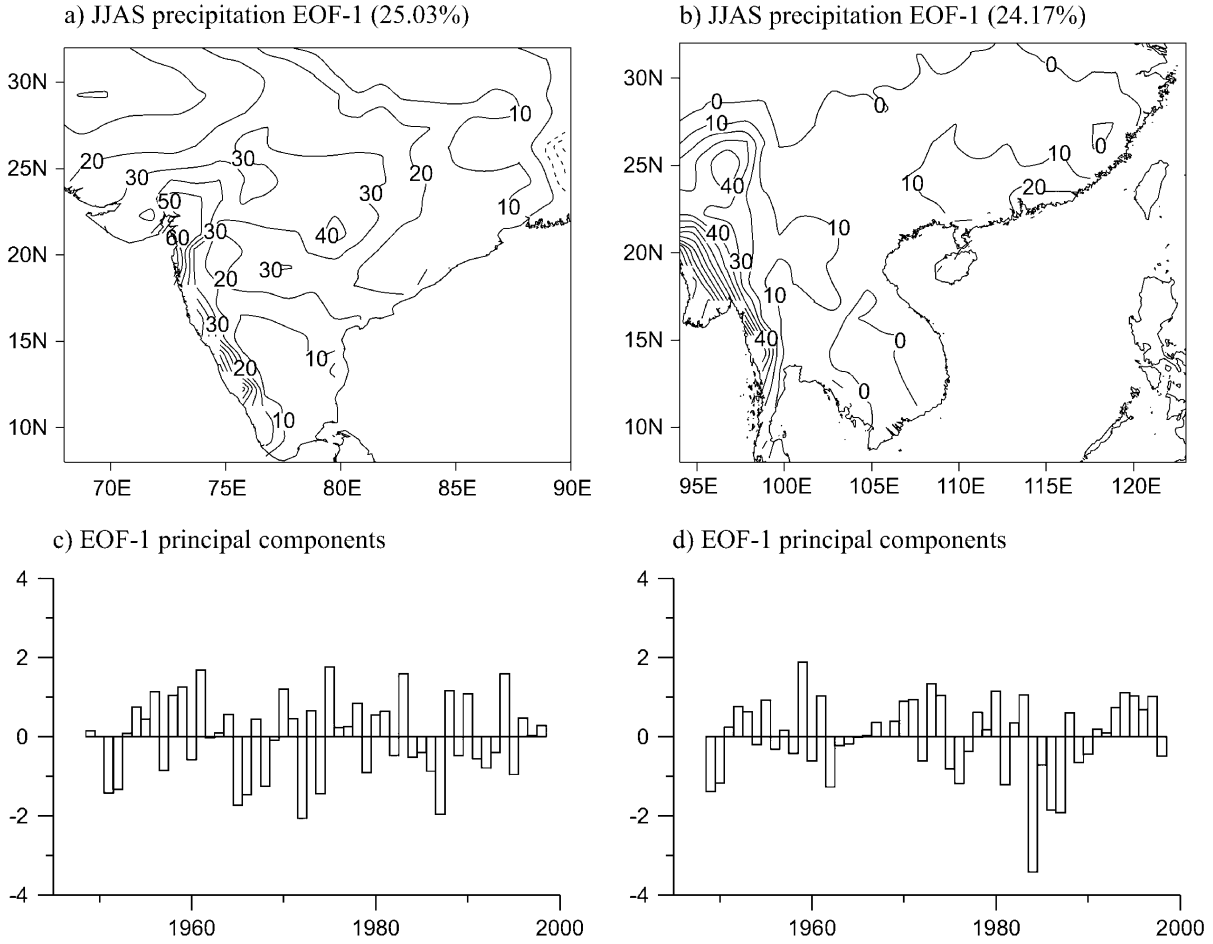

Figure 2. Spatial patterns of the first EOF mode of JJAS rainfall in (a) SAM and (b) SEAM, and (c, d) their respective principal components. Principal components are normalized by their standard deviations

total variance of JJAS rainfall over Southeast Asia. Therefore, as in the case of the SAM, the first EOF mode has become stronger during the last five decades. Principal components of this eigenmode exhibit interannual variations (Figure 2(d)) that are essentially different from those in the SAM (Figure 2(c)). This is confirmed by the low (-0.25) and statistically insignificant correlation between the two time series. Correlation with AIRI is also low (0.27) and statistically insignificant according to a t-test (Bendat and Piersol, 1966). It is also evident (Figure 2(d)) that decadal-scale rainfall changes over Southeast Asia become more pronounced during the last two decades, with predominantly dry conditions from 1984 to 1990, and anomalously wet conditions in 1993–97.

Because the very large variability in the relatively small western regions might bias the spatial patterns obtained of the first EOF mode, we verified the coherency of the rainfall variations revealed by estimation of the correlations between the principal components of the first EOF mode and the rainfall fields in the respective regions. The correlation patterns obtained for the SAM and the SEAM are shown in Figure 3(a) and 3(b) respectively. Correlations between principal components of the first EOF mode of the SAM rainfall and JJAS rainfall fields are positive and statistically significant at the 95% confidence level according to the Student's t-test (Bendat and Piersol, 1966) over almost the whole of India (Figure 3(a)). The largest positive correlations (0.5–0.7) are detected over central and western India. Thus, the first EOF mode of the SAM rainfall does, indeed, reflect coherent rainfall variations in the region.

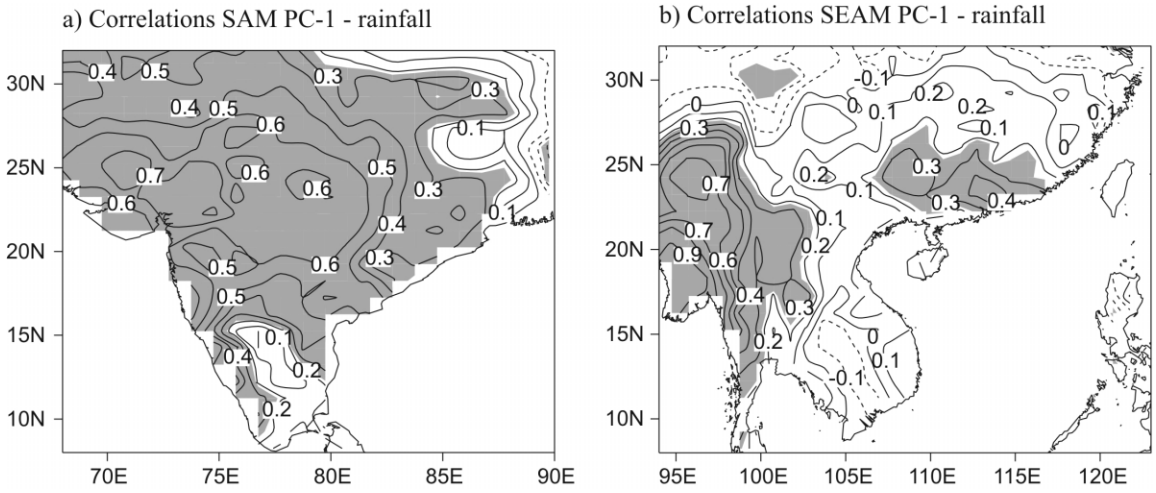

Figure 3. Correlations between (a) SAM JJAS rainfall PC-1 and (b) SEAM JJAS rainfall PC-1 and the rainfall fields over the respective regions. Shaded areas indicate confidence level exceeding 95%

The correlation pattern for the SEAM region (Figure 3(b)) is substantially different from that obtained for the SAM (Figure 3(a)). In general, correlations between principal components of the first EOF mode of the SEAM rainfall and JJAS rainfall fields in this region are lower than those of the corresponding fields over India. Both positive and negative correlations are revealed. However, statistically significant correlations are detected only over the western part of the region (0.6–0.9) and over the southern coast of China (0.3–0.4) (Figure 3(b)). This means that the first EOF mode of the SEAM rainfall reflects rainfall variability over these two sub-regions only. In order to avoid the effect of the large rainfall variability over the western portion of Southeast Asia, we extended the EOF analysis of the SEAM rainfall with the western part being excluded. However, such EOF analysis does not reveal statistically well-separated modes of rainfall variability in the region. Thus, in our analysis, we considered only the first EOF modes of JJAS rainfall, keeping in mind that EOF-1 reflects the rainfall variability over the entire domain in the SAM, but not in the SEAM.

5. RELATIONSHIPS WITH SST VARIATIONS

Figure 4 shows the lead–lag correlations (for time period 1949–1998) between the first principal component of SAM rainfall (PC-1) and monthly SST in the tropical Indian and Pacific Oceans. We correlate the SAM rainfall PC-1 with the SST time series for each month at each grid point beginning with the previous year's September. The areas where the correlations exceed the 95% confidence level are shaded.

As seen in Figure 4, the SST throughout the entire Indian Ocean is positively correlated with the SAM rainfall PC-1 from September (previous year) through to May (monsoon year), confirming the results of earlier studies (Harzallah and Sadourny, 1997; Clark *et al*., 2000). These positive correlations become evidently weaker in April and May (Figure 4(h) and (i)); and, starting from June (Figure 4(j)), negative correlations emerge in the Indian Ocean. However, these correlations become strong (exceeding −0.5) and statistically significant only in September. Though in general agreement, our results are slightly different from those of Clark *et al*. (2000); they analysed correlations between AIRI and seasonal mean SST and detected emerging negative correlations in the subsequent autumn. The difference can be attributed to the different time scales of SST averaging (month in the present study, and season in Clark *et al*. (2000)), a slight difference in the time period analysed (1949–98 in the present study, and 1945–95 in Clark *et al*. (2000)), and the use in the present analysis of the SAM rainfall PC-1 instead of AIRI. On the other hand, we believe that a strong monsoon circulation in the lower troposphere can result in negative SST anomalies in the northern

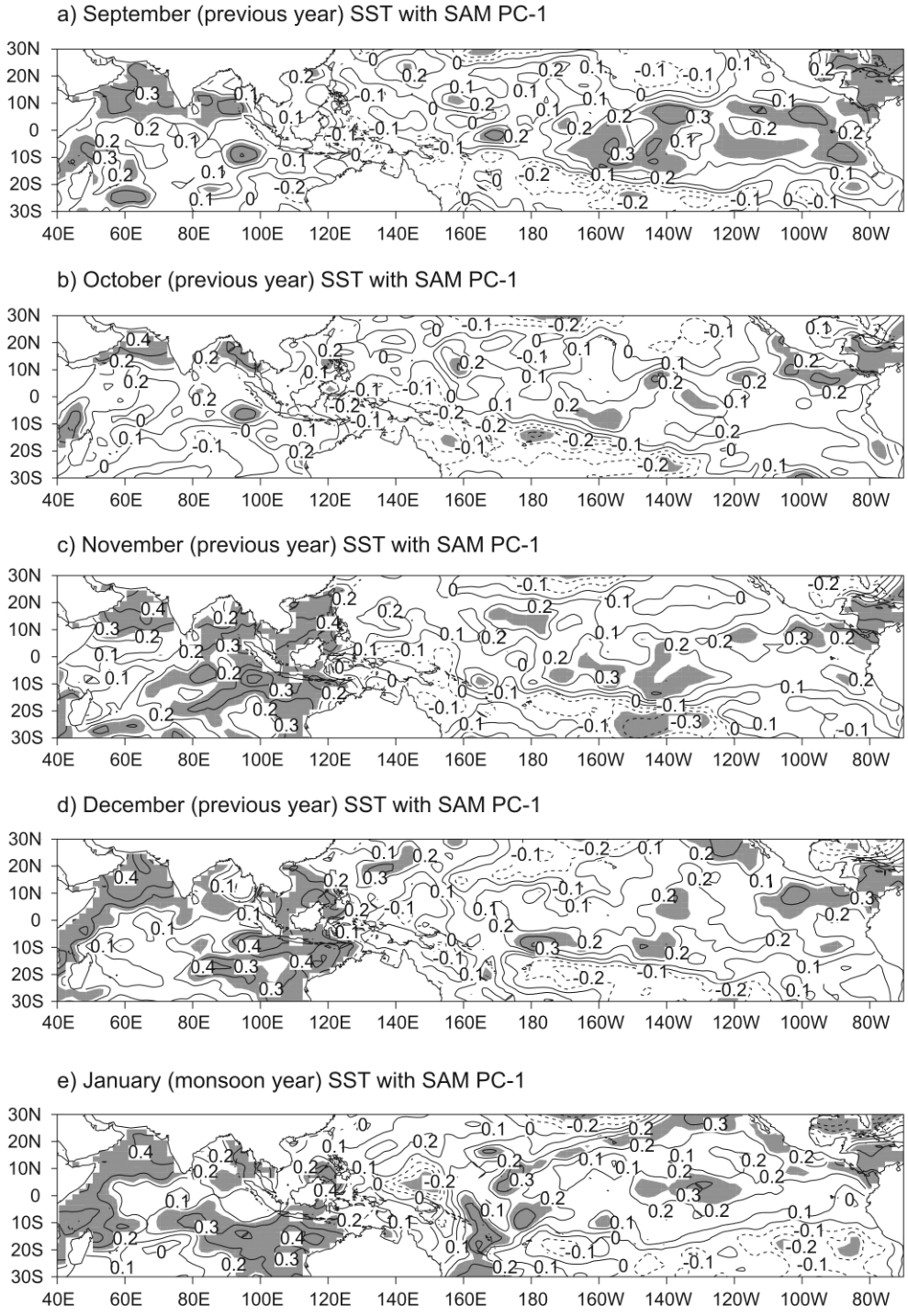

Figure 4. Lead–lag correlations between SAM JJAS rainfall PC-1 and SST in the tropical Indian and Pacific Oceans. Shaded areas indicate confidence level exceeding 95%

Indian Ocean during the monsoon season. In general, the interannual behaviour of the SAM rainfall PC-1 (as presented in Figure 4) shows a quasi-biennial oscillation feature, with the reversal of correlations between

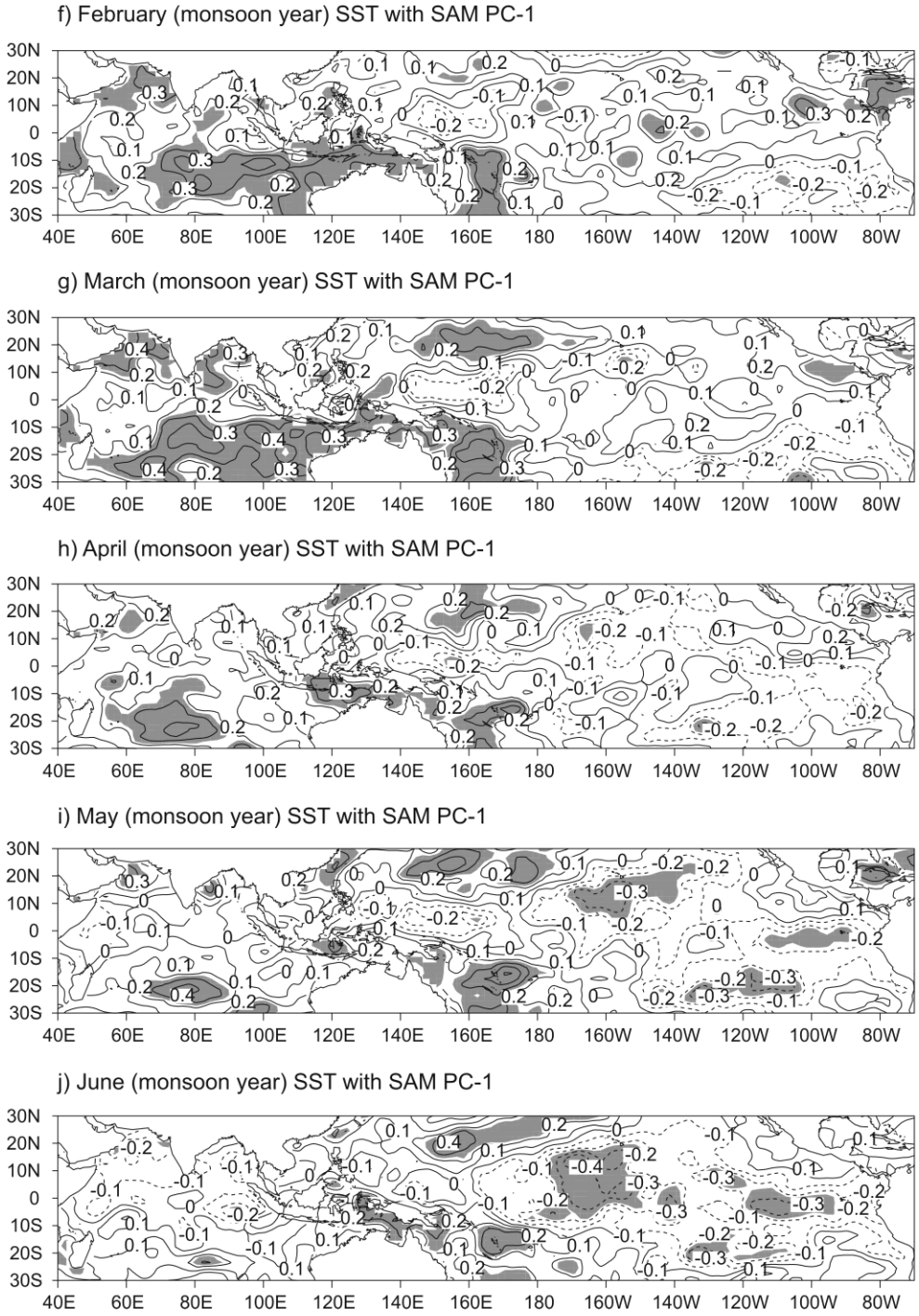

Figure 4. (*Continued*)

months preceding the monsoon and monsoon–post-monsoon months. We note that the biennial nature in the SAM was also detected in other studies (Clark *et al*., 2000; Ailikun and Yasunari, 2001). Thus, the strong SAM rainfall is associated with high SST in the Indian Ocean during the preceding months. Specifically, the strongest correlations are detected during December and January in the northwestern Indian Ocean, where

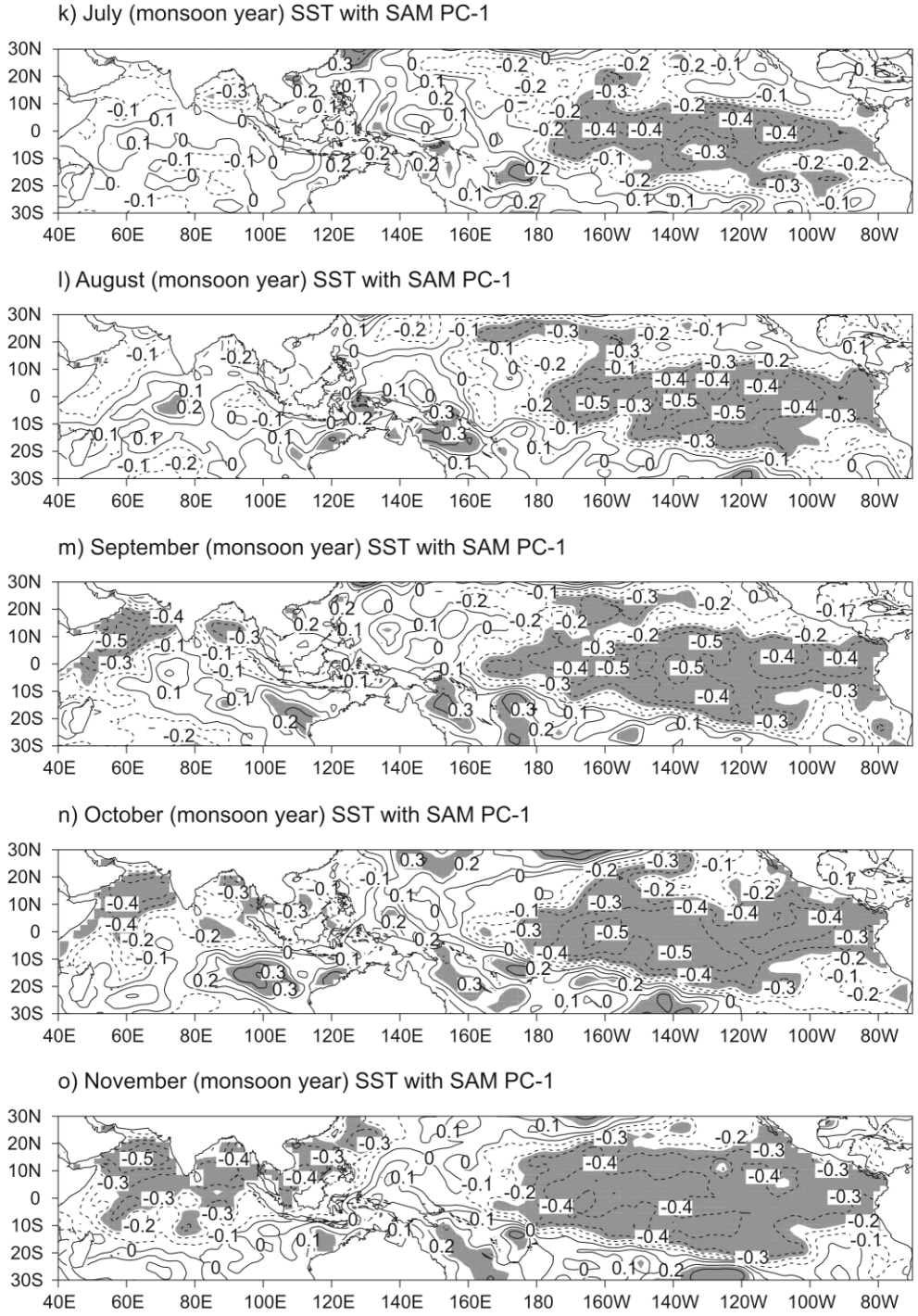

Figure 4. (*Continued*)

they exceed 0.5. Notice that these correlations become essentially weaker during the spring months preceding the SAM. Later, during the monsoon season and subsequent autumn (Figure 4(j)–(o)) the strong SAM is associated with a lower SST in the northern Indian Ocean. This SST cooling may reflect the enhanced

oceanic upwelling along the coast of Somalia and the enhanced evaporation over the Arabian Sea and the Bay of Bengal due to increased monsoon wind. This result agrees with earlier empirical and modelling studies (Shukla, 1987; Rao and Goswami, 1988; Yang and Lau, 1998). Relatively high (exceeding 0.4) and statistically significant positive correlations between SAM rainfall PC-1 and SST are also detected in the eastern–southeastern Indian Ocean during the preceding November–March (Figure 4(c)–(g)). Clark *et al.* (2000) also found high correlations between AIRI and preceding winter SST in this region. We note that weakening of correlations between SAM rainfall PC-1 and SST in the Indian Ocean during spring months can be considered as the regional manifestation of the so-called spring 'predictability barrier'. Earlier, this feature of the tropical climate system was discussed mostly in the context of monsoon–ENSO relationships (e.g. Wright, 1979, 1985; Webster and Yang, 1992; Torrence and Webster, 1998).

Figure 4 shows that the SST over the major portion of the tropical Pacific Ocean is positively correlated with the SAM rainfall PC-1 from September (previous year) through to March (monsoon year). We note, however, that these correlations are relatively low (0.1–0.3) and only marginally significant. Starting from April (Figure 4(h)), negative correlations emerge in the tropical Pacific. These correlations become strong (exceeding -0.4) and statistically significant starting from July. The present negative correlations pattern is similar to the SST pattern observed during La Niña. The strong simultaneous links to ENSO are confirmed by significant correlations with the SOI (0.38) and Niño 3.4 index (-0.48) estimated for the time period 1949–98. Notice that the reversal from positive to negative correlations in the tropical Pacific occurs earlier than that in the Indian Ocean. Although our results demonstrate some agreement with the results of Lau *et al.* (2000), there are important differences. In our study, the cold tongue in the eastern equatorial Pacific SST is not evident in March–May. Indeed, it is formed only during the monsoon season and persists during the subsequent autumn. In contrast to Lau *et al.* (2000), we found strong and statistically significant positive correlations with the preceding winter SST in the Indian Ocean. Also, the positive correlations in the western Pacific during the monsoon season are not as strong as those presented by Lau *et al.* (2000). We believe that the above differences can be attributed to the different SAM indices used. Whereas our SAM rainfall PC-1 reflects rainfall variability over the Indian subcontinent, the SAM index used by Lau *et al.* (2000) includes the convection over the Bay of Bengal that demonstrates somewhat different interannual variability.

Overall, the results presented in this section suggest that the variability of the SAM plays an active rather than a passive role in the SAM–ENSO relationships. The present analysis also suggests that the major precursor signal for SAM is associated with wintertime SST variability in the Indian Ocean.

SST correlations with the SEAM rainfall PC-1 show that SEAM is associated with distinctly different SST patterns (Figure 5). Enhanced summer monsoon rainfall over Southeast Asia is preceded by a high SST in the northern Indian Ocean and the South China Sea in January and February (Figure 5(e) and (f)). Specifically, high correlations (exceeding 0.4) between SEAM rainfall PC-1 and SST are detected in the Arabian Sea in January. In other months, correlations in the region are either marginally significant or insignificant. Note, whereas significant correlations with winter SST in the Arabian Sea are detected for both monsoon subsystems, significant correlations with winter SST in the southeastern Indian Ocean are revealed only for the SAM; likewise, high and significant correlations with winter SST in the South China Sea are detected only for the SEAM. We note that, in contrast to the SAM, there is no reversal evident from positive to negative correlations during the monsoon season. The most prominent features in the Pacific Ocean are the positive correlations in the central tropical Pacific and the negative correlations in the subtropical North Pacific Ocean that form two zonally elongated action centres persisting from the previous November through to March (Figure 5(c)–(g)). When the domain of analysis is extended to the North Pacific extratropics (Figure 6), it becomes evident that the above correlations represent a tripole pattern with the third action centre (positive correlations) located in the central-western North Pacific along approximately 40 °N (Kuroshio Current region). The strongest correlations (exceeding 0.4) in this region are detected in the preceding December–February (Figure 6(a)–(c)). During the following months, the correlations and the whole tripole pattern become weaker. Starting from April (Figure 6(e)), this pattern is hardly discernible. We note that our results are essentially different to the results of Lau

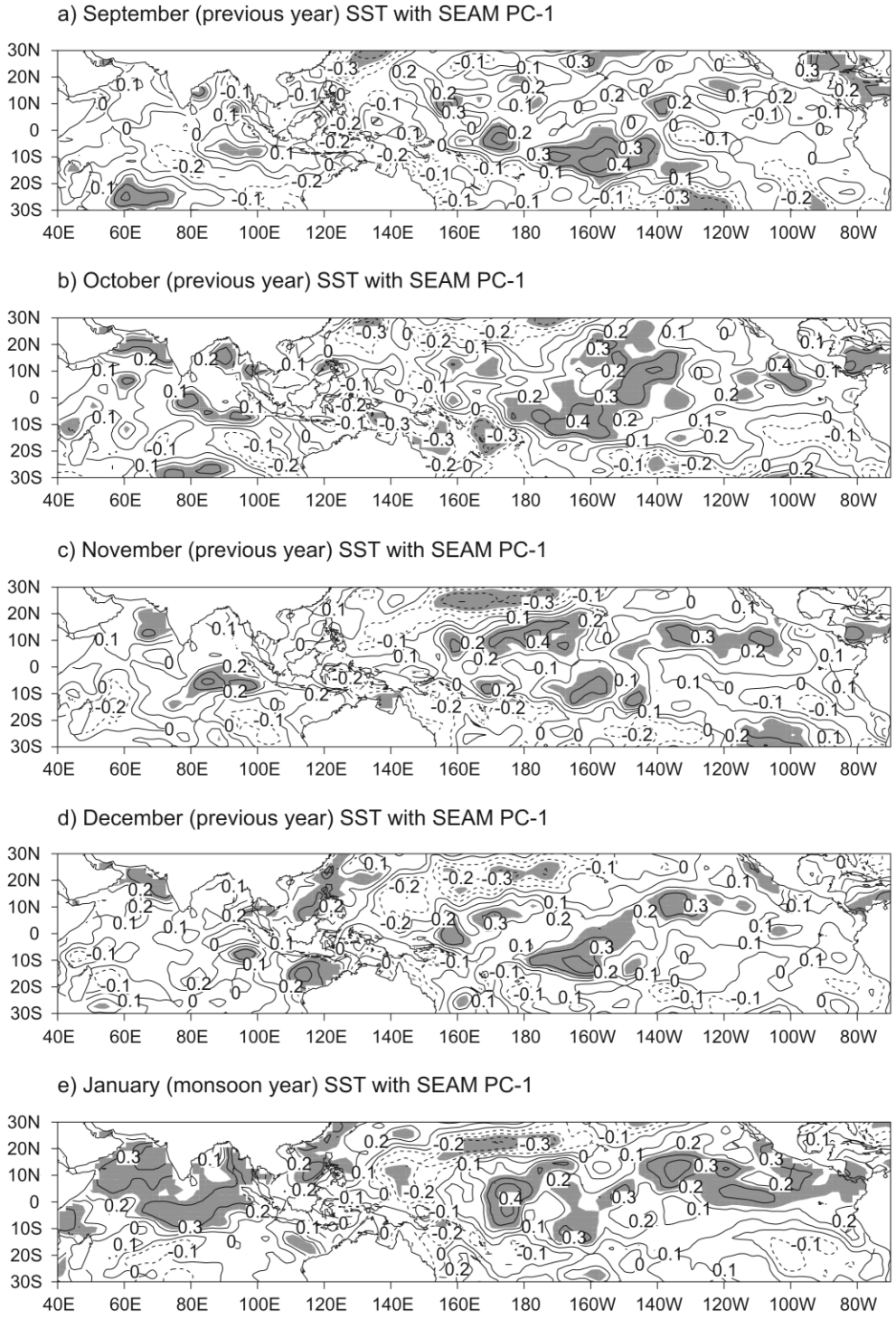

Figure 5. Lead–lag correlations between SEAM JJAS rainfall PC-1 and SST in the tropical Indian and Pacific Oceans. Shaded areas indicate confidence level exceeding 95%

et al. (2000). When analysing links between the SEAM index and seasonal SST anomalies, Lau *et al.* (2000) did not find statistically significant correlations in the Indian Ocean during the winter and spring

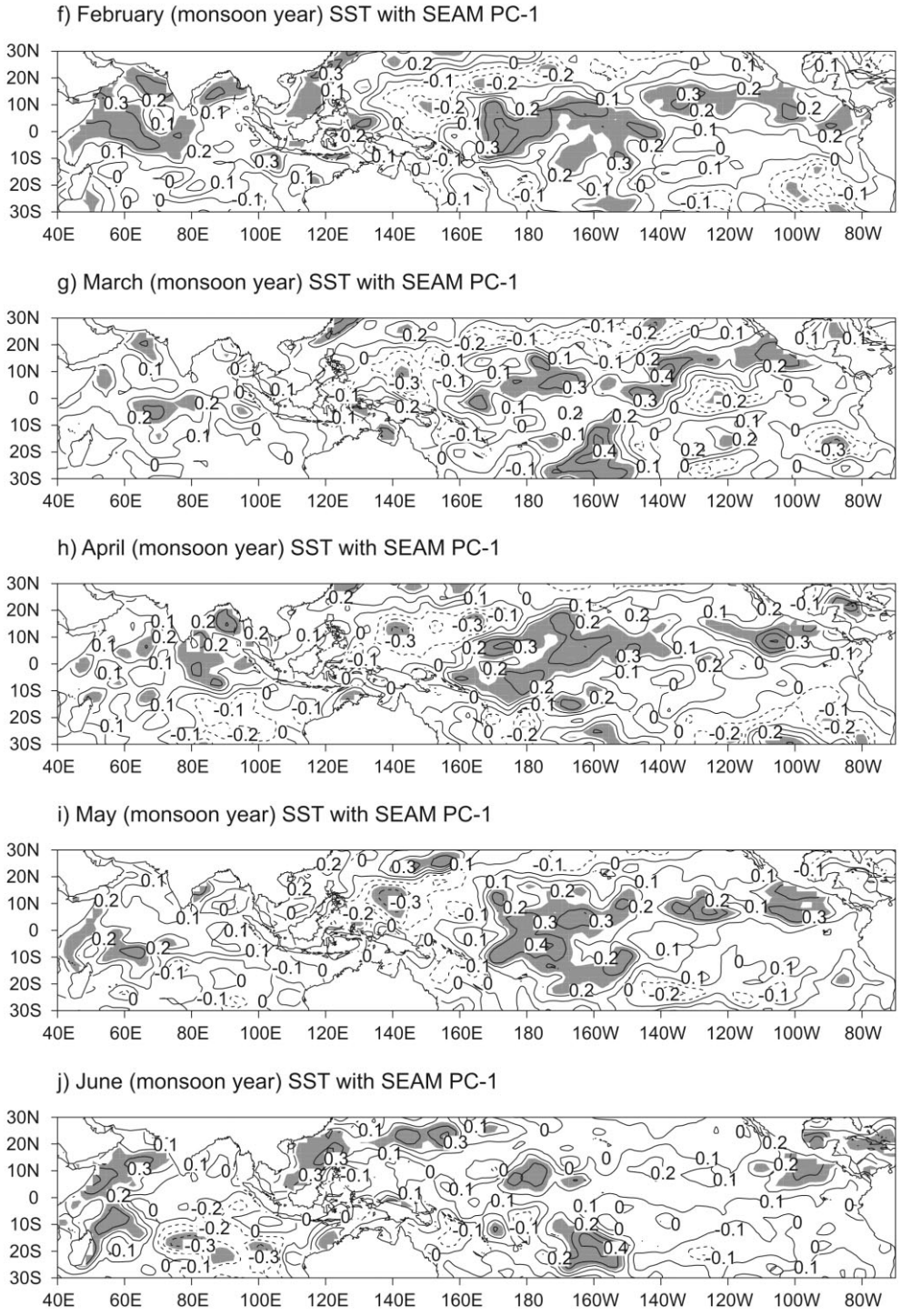

Figure 5. (*Continued*)

preceding the SEAM. In the Pacific Ocean during the same seasons they detected a dipole pattern, whereas correlations in the Kuroshio Current region were not significant (see their figure 12). Furthermore, whereas the present study's wintertime tripole pattern weakens during spring, the wintertime dipole detected

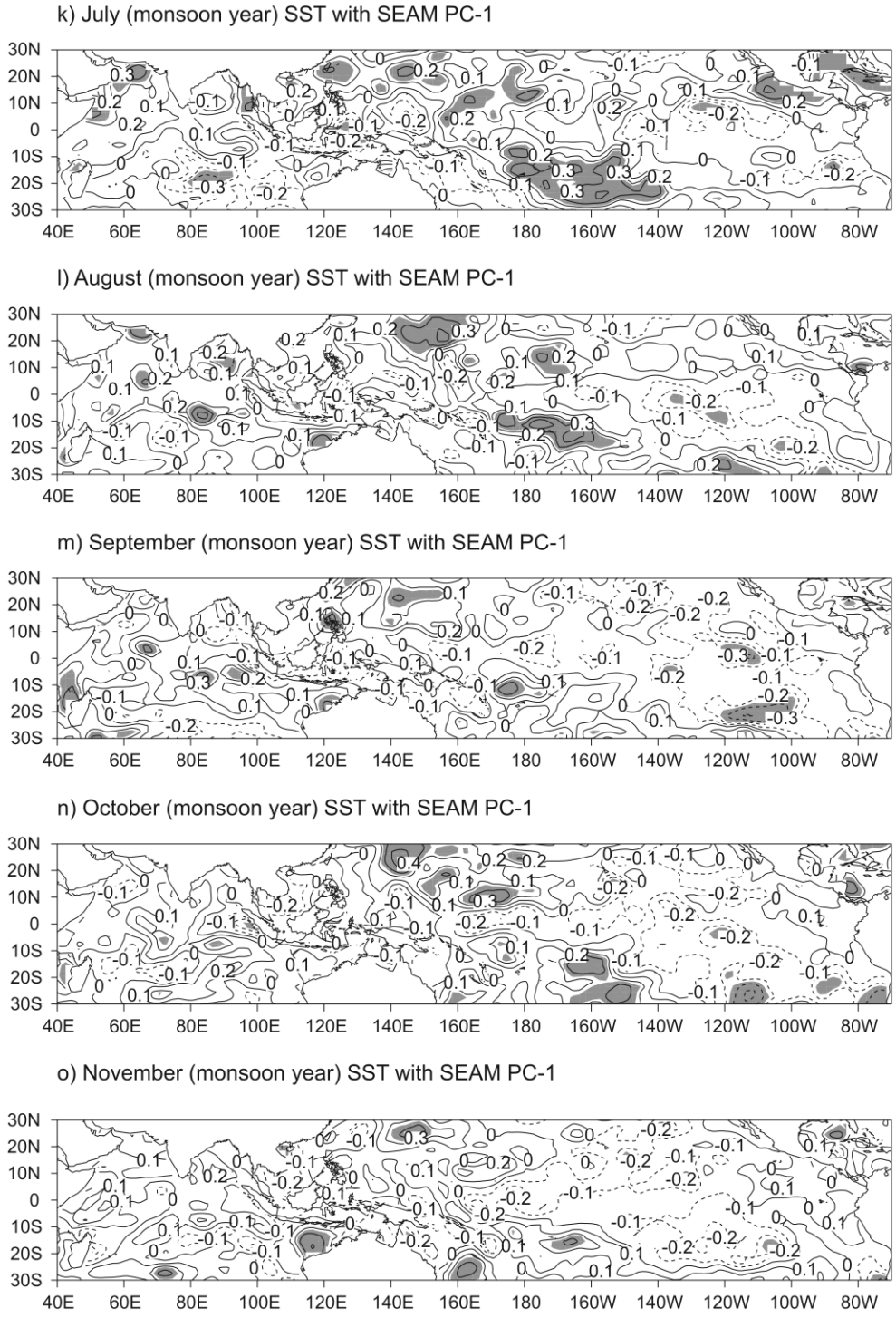

Figure 5. (*Continued*)

by Lau *et al*. (2000) strengthens during spring. Possible reasons for these differences will be discussed below.

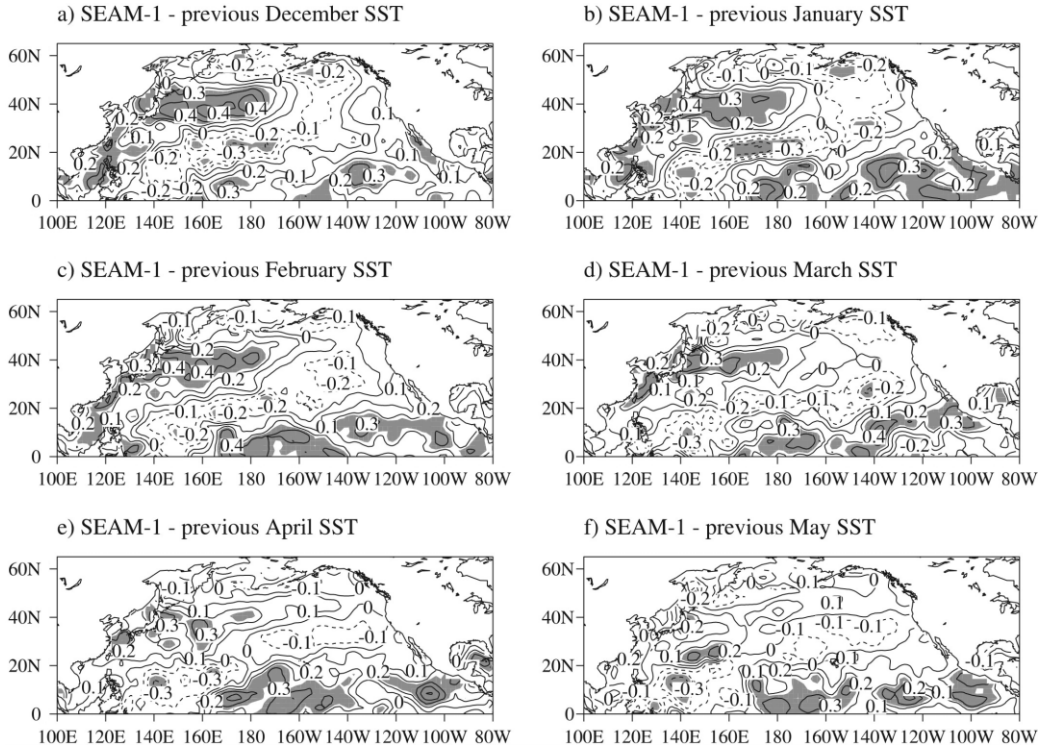

Figure 6. Correlations between SEAM JJAS rainfall PC-1 and SST in the North Pacific Ocean. Shaded areas indicate confidence level exceeding 95%

6. CONCLUDING REMARKS

We analysed the variability of the summer (JJAS) rainfall of the SAM and the SEAM and their relationships with SST variations in the Indian and Pacific Oceans. In general, the total year-to-year rainfall variability expressed by the STD of JJAS rainfall agrees with the rainfall climatology. In other words, the maxima detected in rainfall variability coincide with the maxima of seasonal mean rainfall. Estimated linear trends demonstrate a general level of rainfall decrease over a major portion of India during the last half century, which is most pronounced over northeastern India. Our analysis did not reveal any statistically significant rainfall trend over Southeast Asia.

The leading EOF modes explain about 25% of total rainfall variability in both regions. However, whereas EOF-1 reflects coherent rainfall variability over the entire monsoon domain in the SAM, it does not in the SEAM. As seen from the low correlation between the SAM and SEAM rainfall PC-1 time series, the leading EOF modes of JJAS rainfall over India and over Southeast Asia demonstrate quite different temporal behaviours. In displaying an interannual behaviour very similar to that of AIRI, the SAM rainfall PC-1 can be considered merely as an objectively defined substitute for AIRI. On the other hand, we believe that despite the limitations indicated, the SEAM rainfall PC-1 can be used in further studies as a very useful objectively defined index of the regional rainfall variability. We note that the previously constructed SEAM indices were based on the other climatic variables (see Section 1).

Analysis of the lead–lag correlations between the SAM rainfall PC-1 and SST and between the SEAM rainfall PC-1 and SST revealed that rainfall variability of the two monsoon systems is associated with distinctly different SST patterns. The SAM rainfall is positively correlated with Indian Ocean SST during the preceding months from September (previous year) through to May (monsoon year). Specifically, significant positive correlations are found in the Arabian Sea and in the region northwest of Australia. During the monsoon season, correlations in the Indian Ocean change sign and, starting in September, negative correlations become

statistically significant. Thus, the interannual behaviour of the SAM rainfall shows a quasi-biennial oscillation feature, with a reversal of the correlations between the months preceding monsoon and the monsoon–post-monsoon months. Concerning links to SST variations in the Indian Ocean, our results, in general, support and complement the results of earlier studies (Harzallah and Sadourny, 1997; Clark *et al*., 2000). It is noted that the weakening of correlations between the SAM rainfall PC-1 and SST in the Indian Ocean during the spring months, and the subsequent change of sign of correlations, can be viewed as the regional manifestation of the so-called spring 'predictability barrier'. Earlier, this feature was discussed mostly in the context of monsoon–ENSO relationships (e.g. Wright, 1979, 1985; Webster and Yang, 1992; Torrence and Webster, 1998). In particular, Wright (1979, 1985) has shown that this spring barrier involves a drop of persistence in central Pacific precipitation, eastern Pacific SST, SOI and other ENSO indices. Our results suggest that the spring 'predictability barrier' exists not only in the Pacific, but also in the Indian Ocean.

We did not find statistically significant correlations between the SAM rainfall PC-1 and SST in the tropical Pacific Ocean during the months preceding the SAM. The SAM rainfall is negatively correlated with SST in the central-eastern equatorial Pacific Ocean during the monsoon season and the following autumn, supporting the notion that the SAM plays an active role in ENSO–monsoon relationships.

The SEAM rainfall is positively correlated with SST in the northern Indian Ocean and the South China Sea in the previous January and February. In the Pacific Ocean, significant correlations form a tripole pattern that persists from the previous November through to March. Zonally elongated centres of action of this pattern are located in the tropical, subtropical and extratropical North Pacific Ocean, suggesting that the tropics–extratropics interaction during boreal winter may play an important role in the interannual variability of the SEAM rainfall. As we already noted, these results are different to those presented by Lau *et al*. (2000). There are several reasons that could cause these differences. To construct the SEAM index, Lau *et al*. (2000) used data from the zonal wind at the 200 hPa level. Therefore, their SEAM index reflects the dynamical side of the SEAM. However, if affected by processes in the lower troposphere and by local orography, then the monsoon rainfall may demonstrate interannual variability that differs from that presented by a dynamical index. Another possible reason for the different results is that in the Lau *et al*. (2000) analysis the SEAM domain includes not only Southeast Asia (as in the present study), but also the South China Sea/western Pacific region. This certainly could affect the results of the analysis.

Taking into account the fact that the links detected to the preceding autumn and winter SST in the Indian Ocean essentially weaken during the preceding spring, it is difficult, at this stage, to propose a mechanism explaining how the autumn and winter SST can influence the summer monsoon rainfall. This is also true concerning relationships between SEAM rainfall and wintertime SST in the North Pacific Ocean. Therefore, further observational and modelling studies are needed in order to determine such mechanisms.

ACKNOWLEDGEMENTS

This research was supported by the Russian Foundation for Basic Research, grant 02-05-64498. The CRU05 data were supplied by the Climate Impacts LINK Project (UK Department of the Environment, contract EPG 1/1//16) on behalf of the Climatic Research Unit, University of East Anglia. We thank Steve Worley of the National Center for Atmospheric Research for making the GISST data available to us. The manuscript was improved by the comments of anonymous reviewers.

REFERENCES

Ailikun B, Yasunari T. 2001. ENSO and Asian summer monsoon: persistence and transitivity in the seasonal march. *Journal of the Meteorological Society of Japan* **79**: 145–159.

Allan RJ, Lindesay JA, Reason CJ. 1995. Multidecadal variability in the climate system over the Indian Ocean region during the austral summer. *Journal of Climate* **8**: 1853–1873.

Bendat JS, Piersol AG. 1966. *Measurement and Analysis of Random Data*. John Wiley: New York.

Chang CP, Krishnamurti TN (eds). 1987. *Monsoon Meteorology*. Oxford University Press: Oxford.

Clark CO, Cole JE, Webster PJ. 2000. Indian Ocean SST and Indian summer rainfall: predictive relationships and their decadal variability. *Journal of Climate* **13**: 2503–2519.

Fein JS, Stephens PL (eds). 1987. *Monsoons*. John Wiley: New York.

Gadgil S. 1996. Climate change and agriculture — an Indian perspective. In *Climate Variability and Agriculture*, Abool YR, Gadgil S, Pant GB (eds). Narosa: New Delhi, India; 1–18.
Harzallah R, Sadourny R. 1997. Observed lead–lag relationships between Indian summer monsoon and some meteorological variables. *Climate Dynamics* **13**: 635–648.
Ju J, Slingo JM. 1995. The Asian summer monsoon and ENSO. *Quarterly Journal of the Royal Meteorological Society* **122**: 1133–1168.
Kripalani RH, Kulkarni A. 1997. Rainfall variability over south-east Asia — connections with Indian monsoon and ENSO extremes: new perspectives. *International Journal of Climatology* **17**: 1155–1168.
Krishnamurthy V, Shukla J. 2000. Intraseasonal and interannual variability of rainfall over India. *Journal of Climate* **13**: 4366–4377.
Lau K-M. 1998. A climate system approach to studies of the Asian summer monsoon. In *Extended Abstracts, International Conference on Monsoon and Hydrologic Cycle*, Kyongju, Korea. Korean Meteorological Society: 15.
Lau K-M, Bua W. 1998. Mechanism of monsoon–southern oscillation coupling: insights from GCM experiments. *Climate Dynamics* **14**: 759–779.
Lau K-M, Kim K-M, Yang S. 2000. Dynamical and boundary forcing characteristics of regional components of the Asian summer monsoon. *Journal of Climate* **13**: 2461–2482.
New MG, Hulme M, Jones PD. 1999. Representing twentieth-century space–time climate variability. Part I: development of a 1961–90 mean monthly terrestrial climatology. *Journal of Climate* **12**: 829–856.
New MG, Hulme M, Jones PD. 2000. Representing twentieth-century space–time climate variability. Part II: development of a 1901–96 monthly grids of terrestrial surface climate. *Journal of Climate* **13**: 2217–2238.
Nicholls N. 1983. Predicting Indian monsoon rainfall from sea surface temperature in the Indonesia–north Australia area. *Nature* **306**: 576–577.
Normand C. 1953. Monsoon seasonal forecasting. *Quarterly Journal of the Royal Meteorological Society* **79**: 463–473.
North GR, Bell TL, Calahan RF. 1982. Sampling errors in the estimation of empirical orthogonal functions. *Monthly Weather Review* **110**: 699–706.
Parker DE, Folland CK, Jackson M. 1995. Marine surface temperature: observed variations data requirements. *Climatic Change* **31**: 559–600.
Parthasarathy B, Munot AA, Kothawale DR. 1988. Regression model for estimation of Indian food grain production from Indian summer rainfall. *Agricultural and Forecasting Meteorology* **42**: 167–182.
Parthasarathy B, Kumar KR, Kothawale DR. 1992. Indian summer monsoon rainfall indices: 1871–1990. *Meteorological Magazine* **121**: 174–186.
Parthasarathy B, Munot AA, Kothawale DR. 1994. All-India monthly and seasonal rainfall series: 1871–1993. *Theoretical and Applied Climatology* **49**: 217–224.
Rao KG, Goswami BN. 1988. Interannual variations of sea surface temperature over the Arabian Sea and the Indian monsoon: a new perspective. *Monthly Weather Review* **116**: 558–568.
Rayner NA, Folland CK, Parker DE, Horton EB. 1995. A new global sea-ice and sea surface temperature (GISST) data set for 1903–1994 for forcing climate models. Internal Note 69, Hadley Centre, UK Meteorological Office. [Available from Meteorological Office, London Road, Bracknell RG12 254, UK].
Ropelewski CF, Jones PD. 1987. An extension of the Tahiti–Darwin southern oscillation index. *Monthly Weather Review* **115**: 2161–2165.
Sadhuram Y. 1997. Predicting monsoon rainfall and pressure indices from sea surface temperature. *Current Science* **72**: 166–168.
Shukla J. 1987. Interannual variability of monsoons. In *Monsoons*, Fein JS, Stephens PL (eds). John Wiley and Sons: 399–464.
Shukla J, Mooley DA. 1987. Empirical prediction of the summer monsoon rainfall over India. *Monthly Weather Review* **115**: 695–703.
Torrence C, Webster PJ. 1998. The annual cycle of persistence in the El Nino/southern oscillation. *Quarterly Journal of the Royal Meteorological Society* **124**: 1985–2004.
Torrence C, Webster PJ. 1999. Interdecadal changes in the ENSO–monsoon system. *Journal of Climate* **12**: 2679–2690.
Trenberth KE. 1984. Signal versus noise in the southern oscillation. *Monthly Weather Review* **112**: 326–332.
Trenberth KE. 1997. The definition of El Nino. *Bulletin of the American Meteorological Society* **78**: 2771–2777.
Troup AJ. 1965. The southern oscillation. *Quarterly Journal of the Royal Meteorological Society* **91**: 490–506.
Von Storch H, Navarra A. 1995. *Analysis of Climate Variability*. Springer-Verlag: New York.
Wang B, Fan Z. 1999. Choice of South Asian summer monsoon indices. *Bulletin of the American Meteorological Society* **80**: 629–638.
Webster PJ, Yang S. 1992. Monsoon and ENSO: selectively interactive systems. *Quarterly Journal of the Royal Meteorological Society* **118**: 877–926.
Webster PJ, Magana VO, Palmer TN, Shukla J, Tomas RA, Yanai M, Yasunari T. 1998. Monsoons: processes, predictability, and the prospects for prediction. *Journal of Geophysical Research* **103**: 14 451–14 510.
Wilks DS. 1995. *Statistical Methods in the Atmospheric Sciences*. Academic Press: San Diego.
Wright P. 1979. Persistence of rainfall anomalies in the central Pacific. *Nature* **277**: 371–374.
Wright P. 1985. The southern oscillation: an ocean–atmosphere feedback system? *Bulletin of the American Meteorological Society* **66**: 398–412.
Yang S, Lau K-M. 1998. Influences of sea surface temperature and ground wetness on the Asian summer monsoon. *Journal of Climate* **11**: 3230–3246.

